Eur. Phys. J. D **11**, 99–108 (2000)

THE EUROPEAN PHYSICAL JOURNAL D

EDP Sciences

Diode laser spectroscopic measurement and impact theoretical analysis of collision broadening of acetylene ($\nu_1 + 3\nu_3$) band transitions

B.K. Dutta, D. Biswas, B. Ray, and P.N. Ghosh[a]

Department of Physics, University of Calcutta, 92 A.P.C. Road, Calcutta 700 009, India

Received 24 November 1999

Abstract. A near infrared diode laser spectrometer has been used for measurement of line shapes of the rotational transitions of the ($\nu_1 + 3\nu_3$)overtone-combination band of acetylene perturbed by oxygen and air. Pressure-broadening coefficients and line strength parameters are extracted from least squares fitting of the spectra with Voigt profiles. A detailed calculation of pressure-broadening coefficients for the self, nitrogen and oxygen broadening cases has been performed by using semi-classical impact theory based on quadrupolar and dispersion interactions. The relative importance of the intermolecular interactions has been investigated and it is found that for these weak interaction cases dispersive terms have a dominant role in line broadening. This is more pronounced for the O_2-broadening case. We have included all the non-resonant terms till convergence is achieved. The cutoff parameter b_0 of the Anderson procedure has been determined separately for each non-resonant process. In order to include the orientation effect of the molecules at the moment of collision we have considered an average kinetic collision diameter which sets the lower limit of b_0. This improves the result considerably and the calculated values are close to the observed results. The J-dependence of the half width is also reported and shows decrease for large J-values.

PACS. 42.62.Fi Laser spectroscopy – 33.70.-w Intensities and shapes of molecular spectral lines and bands – 33.70.Jg Line and band widths, shapes, and shifts

1 Introduction

The broadening of spectral lines provides important information for intermolecular interactions and also leads to useful results for analysis of spectroscopic data of molecules of atmospheric and astrophysical interest. Recent availability of very narrow line width tunable laser sources and improved techniques for high sensitivity detection allow measurement of line shape with high precision. A careful delineation of the observed spectral line can lead to apportioning of the resultant line shape to different broadening mechanisms. If the pressure broadening component of the observed line shape in presence of self and foreign gas perturbers can be isolated it is possible to investigate the line broadening caused by the intermolecular Coulombic potential leading to multipolar, dispersion and induction interactions.

In a calculation of line width the role of different multipolar interactions in the intermolecular potential [1] should be investigated. Robert *et al.* [2] showed that the effects of all the terms in the potential are not additive and derived the contributions of various terms of the potential to the collisional probability function $S_2(b)$ as a function of impact parameter b. Since $S_2(b)$ is a probability function its maximum value is unity for a certain value of b referred as b_0. In the pressure broadening theories [3,4] the value of b_0 plays a crucial role in line width calculation. In the case of collision with different molecules and also for self-collision in the vibrational transition case there are no exactly resonant terms and the effect of these non-vanishing non-resonance terms should be investigated. So the value of b_0 is to be evaluated for each individual non-resonant process separately.

Semiconductor diode lasers with very narrow line width can be tuned over small spectral ranges suitable for line shape studies. It has been shown [5] that the second derivative spectra obtained using source modulation technique have enhanced sensitivity which enables measurement of weak overtone transitions. Recently we reported line broadening measurements of rotational components of the ($\nu_1 + 3\nu_3$) band of acetylene in presence of self and N_2 perturbers by a diode laser spectrometer [5].

Acetylene molecule has been observed in the atmospheres of the planets Jupiter, Saturn and its satellite, Titan [6–8]. It is a trace constituent of the earth's atmosphere and could play an important role in the global climate in the not so far future due to the increased use of automobiles worldwide [8]. Overtone spectra of this prototype of non-polar linear polyatomic molecules in the

[a] e-mail: png@cucc.ernet.in

visible to near infrared region were studied photographically in the 1930s, as reviewed by Herzberg [9]. The $(\nu_1 + 3\nu_3)$ band system of acetylene with ν_1 as the symmetric CH stretch and ν_3 as the antisymmetric stretch has been studied by ring dye laser spectroscopy [10], interferometric technique [11], photoacoustic spectroscopy with Ti:sapphire ring dye laser [12] and diode laser spectroscopy [13,14].

The shape of a spectral profile depends on various line broadening mechanisms. Most line shape analysis in the intermediate range of pressure where both the Doppler and the collisional dephasing effects are significant are satisfactorily done by the standard Voigt profile, a convolution of the Lorentz and the Gauss curves, which has the correct limiting behaviour at high and low pressures. However, in some special cases the molecular collisions perturb the translational motion of the molecules if the rotational energy difference $\Delta E(J)$ is such that collisions do not perturb the phase of the emitted radiation. In such cases the Doppler component in the Voigt profile becomes pressure dependent resulting in a Dicke-narrowed profile [15].

In this paper we report diode laser spectroscopic measurement of collision broadening coefficients and line strength parameters for the six rotational transitions of the $(\nu_1 + 3\nu_3)$ band of acetylene in the presence of oxygen and air. To our knowledge oxygen and air-broadening measurements of this near infrared combination overtone band have not been published so far. We also report detailed calculation of the self, N_2 and O_2 broadening coefficients of acetylene overtone spectra on the basis of semi-classical impact model and compare them with our observed values. The air-broadening coefficients are also computed from the N_2 and O_2 broadening coefficients. The effects of the different intermolecular interactions on the collision broadening have been studied.

2 Experimental

The apparatus used for the measurements is shown schematically in Figure 1. The GaAlAs semiconductor laser diode HL7838G supplied by Hitachi has a standard wavelength range of 770–795 nm with a typical value of 780 nm. The limiting drive current for diode is 70 mA and the temperature range used for the wavelength scanning is 26–50 °C. Peltier elements are used for heating and cooling. The diode laser emission wavelength shows a linear temperature dependence (0.084 nm/°C). In the free running mode short term ripples of the diode are 10 MHz or less for a period of a few seconds. Long term frequency stability of the laser is controlled by the long term temperature stability which is better than 10 mK at any operating temperature leading to an wavenumber stability of better than 0.01 cm^{-1} for a period of hours. The measurement for one particular transition covering nearly 10 GHz around any peak takes approximately 5 s. So the measurement precision is better than 0.003 cm^{-1}. The low noise current source driving the laser has a linear wavenumber dependence of 0.1 cm^{-1}/mA. The long

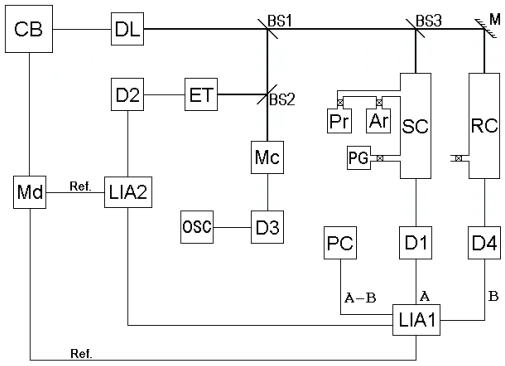

Fig. 1. Schematic of the NIR diode laser spectrometer; DL: diode laser, CB: control box, ET: etalon, BS: beam splitter, M: mirror, MC: monochromator, Md: modulator, D: detector, LIA: lock-in amplifier, PC: personal computer, SC: sample cell, RC: reference cell, PG: pressure gauge, OSC: oscilloscope, Ar: absorber gas, Pr: perturber gas.

term drift of the current is less than 10 ppm. The measurement cell used in this work is a cylindrical glass cell of 1.5 m path length and 5 cm diameter. The laser probe passes through the sample cell and the output is then focussed onto a UDT 455 silicon photodetector working under ambient temperature condition. An Oriel monochromator is employed to get the rough wavelength reading. A part of the laser radiation from the beam splitter is fed to another photodetector through an air-spaced etalon (finesse = 36) from TecOptics for simultaneous recording of the etalon fringes spaced 5.00 GHz apart. This helps in calibrating the frequency scan with a precision of 10 MHz. For absorption spectroscopy of the weak combination overtone transitions the source modulation technique has been adopted. For the "in-phase" detection a sinusoidal modulation at a frequency of 5 kHz supplied by an external signal generator, which also supplies the reference signal to the lock-in amplifier, is added to the diode laser injection current. The transmitted power collected by the photodetector is sent to the lock-in amplifier SR530 with a time constant of 100 ms interfaced to a personal computer (PC–AT 386) *via* RS232–C in order to extract the second harmonic signals. The *2f* detection procedure produces negligible DC offset and reduces the effect of laser power fluctuations. Furthermore, the fact that *2f* signal swings around zero facilitates subsequent signal analysis. The modulation amplitude ω_m has been adjusted so as to give the largest signal with no undue broadening of the line. The amplitude of the modulating signal corresponds to a frequency modulation of 10 MHz which is negligibly small compared to the measured line width which is nearly 450 MHz arising from the Doppler broadening or even larger than that. Hence the phase sensitive detected output is the undistorted second derivative of the true absorption spectrum [16]. Generally, a modulation amplitude upto 5% of the measured line width can be used without any distortion of the measured line profile. The modulation of the diode injection current at kHz

frequencies can usually remove the effect of any slope in the background spectrum which may hinder the observation of weak signals [17]. The value of the ratio of peak to peak value of a typical signal to rms noise is nearly 51. Before each recording the second derivative spectrum of the evacuated sample cell has been measured to ensure uniform flat baseline. The underived background spectrum is also measured in an empty cell with the help of a mechanical chopper. This shows that the baseline of the absorption spectrum is constant across a measured transition frequency. A constant laser power of 3.5 mW is used for all the line shape measurements. The DC level of the input beam in the empty cell is monitored in an oscilloscope in order to obtain the incident laser power. Commercial acetylene gas with natural isotopic abundance is used without further purification. Oxygen is procured from Aldrich and has a stated purity of 99.6+ % while standard laboratory air has been used. All the measurements are recorded at room temperature, 300 ± 1 K.

Measurements with the diode laser revealed all the transitions of the $(\nu_1 + 3\nu_3)$ combination overtone band previously observed by Hedfeld and Lueg [18] and further studied by Lucchesini *et al.* [14]. Accurate measurement of the shape of all the transitions could not be carried out due to the mode hops and power fluctuations of the laser emissions. Usually three to four transitions could be observed in one mode covering a range of 6–7 cm^{-1}. The precisely determined wavenumber differences obtained from the etalon fringes are compared to the wavenumber values listed in the literature [18]. In this process we could assign the transitions. The transitions selected in this work are P7, P8, P13, P15, R9 and R11. The line center frequencies are taken from Hedfeld and Lueg [18]. For each of these six transitions we have recorded the oxygen and air-broadened spectra in the pressure range from 100 torr to 500 torr in steps of 100 torr of the perturber with a fixed absorber pressure of 100 torr. The pressure measurement has been carried out by using MKS Baratron capacitance manometer type 122B with a full scale of 1 ktorr. For the two R-branch transitions in case of air-broadening the line shapes were not well defined for analysis and hence were excluded from the simulation process. It may be noted here that the spectra obtained with air perturber appeared to be more noisy and only a few lines could be retrieved. One reason could be the large number of impurity molecules that might be present in the air used as perturber. The background noise is eliminated by subtracting the empty cell (Fig. 1) second derivative reference spectrum from the corresponding measured sample spectrum before analysis. The observed second derivative line shapes thus obtained appeared to be symmetrical.

3 Line shape analysis

For numerical computation of the spectral lines we have used the Voigt profile which is the real part of the complex probability function and may be expressed as

$$\alpha_V(\omega) \; = A \left(\frac{y}{\pi}\right) \int_{-\infty}^{+\infty} \frac{\exp\left(-\tau^{\,2}\right)}{y^{\,2} + \left(x - \tau\right)^{\,2}} \, \mathrm{d}\tau. \qquad (1)$$

The dimensionless parameters x and y are defined as $x = (\omega - \omega_0)/\sigma$, $y = \Gamma/\sigma$. τ is the dimensionless time parameter and $A = \sqrt{\pi}\, S/\sigma$. Γ is the collisional half width arising from state (or phase) changing collisions, ω_0 is the line center frequency and σ is the calculated Doppler half width at e^{-1} intensity, $\sigma = \omega_0 \sqrt{2\, k_{\mathrm{B}}\, T/m\, c^2}$ at temperature T and m is the molecular mass of the absorber. S is the line strength parameter with the dimension cm/molecule. The standard Voigt profile has been computed following the algorithm developed by Hui *et al.* [19]. The intensity for each line is given by Beer-Lambert's law

$$I(\omega) \; = \; I_0(\omega) \exp\left[\, -\alpha_V(\omega)\, pl \,\right] \qquad (2)$$

where p is the absorber pressure and l is the path length. $I_0(\omega)$ and $I(\omega)$ are the incident and transmitted intensities respectively. To extract the line shape parameters the calculated transmission intensities $I(\omega)$ are fitted with the observed transmission profiles. Since detection is done at the second harmonic of the modulation frequency the original absorption line shapes are recovered by integrating the derivative output. For this purpose the derivative must be very accurately determined, which is possible with a small modulation amplitude ω_{m} as described earlier.

For extraction of the line parameters a non-linear least squares fitting method based on Levenberg-Marquardt procedure [20] is used. In the fitting process the Doppler HWHM $\sigma\sqrt{\ln 2}$ is kept constant at its theoretical value of 0.015 cm^{-1} and the pressure broadening coefficient Γ/P and the line strength parameter S are kept as floating parameters. A simulation of true etalon fringes shows that the observed second derivative etalon fringes contain contributions from the laser line width, slow response from the detector and other factors. A comparison with the simulated fringes leads to an estimated half width of 0.021 cm^{-1} for the laser line width and other factors [21]. We assumed this width arises from homogeneous broadening and hence we convoluted a Lorentzian function having this line width with the calculated spectrum before fitting with the observed spectrum. The fact that $I_0(\omega)$ is constant across the lines and $\alpha_V(\omega)pl$ is much less than 1 for all the transitions the transmitted intensity $I(\omega)$ is proportional to $\alpha_V(\omega)$. The recorded intensities were normalized with respect to the DC level of the empty cell.

In Figure 2 the observed oxygen-broadened spectra for three different broadening gas pressures and a fixed pressure of the absorber are presented together with the residuals giving the difference between the observed and least squares fitted spectra. For all the four$P$-branch and two R-branch transitions measurement and least squares fitting are carried out for five different pressures of the oxygen perturber. A plot of the Γ values obtained from the fit against pressure (Fig. 3) shows linear variation. For the air broadening case measurements have been carried

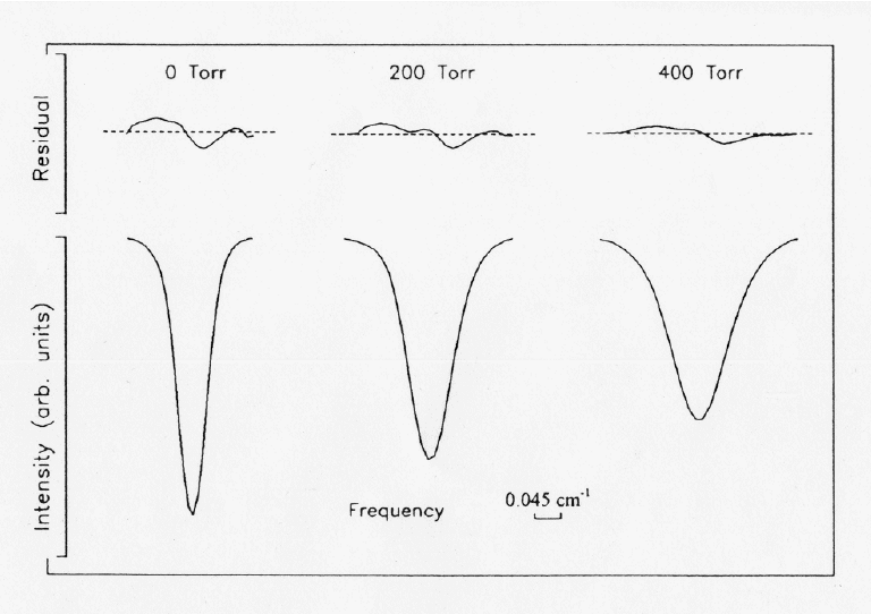

Fig. 2. Line shape of the C_2H_2 ($\nu_1 + 3\nu_3$)band transition P7 (12658.11 cm^{-1}) for different oxygen pressures (shown in the figure) for an absorber pressure of 100 torr. The upper traces plotted in the same scale as the observed line profile show the residuals of the observed and the least squares fitted Voigt profiles.

Table 1. Oxygen and air-broadening coefficients Γ/P ($cm^{-1}atm^{-1}$) and line strength values S (cm/molecule) in the ($\nu_1 + 3\nu_3$) band of C_2H_2[a].

Transition	ω_0[b] (cm^{-1})	S (cm/molecule)		Γ/P ($cm^{-1}atm^{-1}$)						
				oxygen			air			
		oxygen	air	Obs.	Cal.[c]		Obs.		Cal.[c]	
					$q_1 = 3.0$	$q_1 = 4.0$	I[d]	II[e]	$q_1 = 3.0$	$q_1 = 4.0$
P7	12658.11	1.741(11)E–23	1.456(3)E–23	0.0641(10)	0.0477	0.0481	0.0783(2)	0.0769(5)	0.0519	0.0556
P8	12655.37	9.594(6)E–24	7.094(1)E–24	0.0511(1)	0.0487	0.0491	0.0560(5)	0.0584(4)	0.0531	0.0562
P13	12641.15	2.130(31)E–23	4.404(10)E–23	0.0580(4)	0.0521	0.0525	0.0708(6)	0.0703(5)	0.0581	0.0614
P15	12635.18	1.603(39)E–23	4.170(12)E–23	0.0462(1)	0.0522	0.0527	0.0505(4)	0.0517(4)	0.0591	0.0625
R9	12696.42	2.768(27)E–23	—	0.0764(3)	0.0511	0.0515	—	0.0879(4)	0.0562	0.0594
R11	12699.91	3.118(25)E–23	—	0.0736(2)	0.0522	0.0527	—	0.0845(2)	0.0579	0.0611

[a]The numbers in parentheses are one standard deviation, in units of the least significant digits.
[b]The line positions are taken from reference [18].
[c]q_1: Quadrupole moment of acetylene in d Å.
[d]Direct measurement.
[e]Obtained from the N_2- [5] and O_2-broadening measurements by using the relation $\Gamma_{air} = 0.79\,\Gamma_{N_2} + 0.21\,\Gamma_{O_2}$.

out for four P-branch transitions and for four different pressures of the perturber gas. In this case also a linear variation of Γ against P is obtained (Fig. 4). The vertical error bars in Figures 3 and 4 represent the standard errors obtained from computer fitting of the spectral data. These errors are used in the linear fit of data at different pressures to compute mean Γ/P and S (Tab. 1). For the air-broadening case we also present the Γ/P values obtained from those of N_2 and O_2 perturbers. The resultant uncertainties of Γ/P values are somewhat lower than those reported previously [13,14]. The higher accuracy of the Γ/P values results from relatively unperturbed line shape and improved accuracy of the spectral measurement as discussed in Section 2.

The values of Γ/P show a decrease with increasing value of the quantum number J for the P-branch transitions. In case of oxygen broadening the coefficients are consistently lower than the case of self and N_2-broadening measurements [5]. All the observed lines could be fitted by using the standard Voigt profile. This shows that there is no narrowing effect caused by the velocity changing collisions as observed in the case of oxygen A-band spectra [16,22]. This is in agreement with the observations of Lucchesini *et al.* [14]. The pressure broadening coefficients

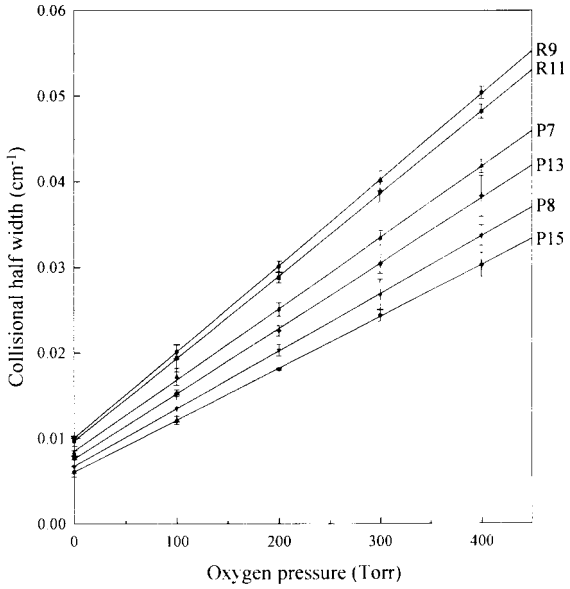

Fig. 3. Collisional half widths of the C_2H_2 $(\nu_1 + 3\nu_3)$band transitions in the presence of O_2 perturber derived from the least squares fitted Voigt profiles. The vertical bars represent the standard errors obtained from the computer fitting.

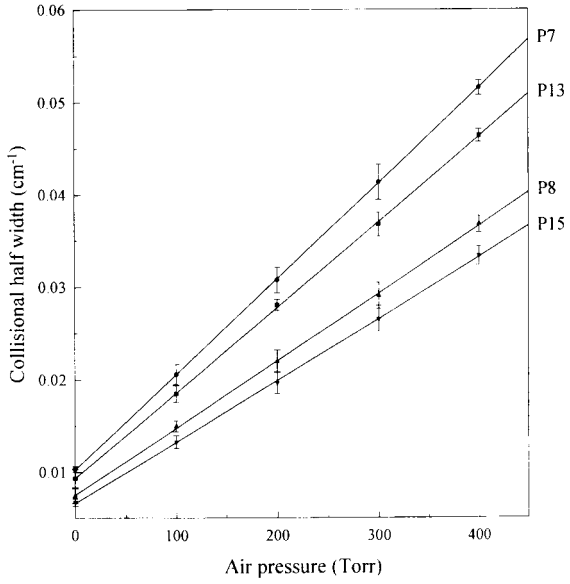

Fig. 4. Collisional half widths of the C_2H_2 $(\nu_1 + 3\nu_3)$band transitions in the presence of air perturber extracted from the least squares fitted Voigt profiles. The vertical bars represent the standard errors obtained from the computer fitting.

obtained for the six transitions are comparable to those of the other rotational transitions for the same vibrational mode $(\nu_1+3\nu_3)$ measured by Lucchesini *et al.* [14] who reported the full width at half maximum values. The mean values of S are comparable with those for the self and nitrogen perturber cases [5]. It is found that the S values show wide variation with change of collision partner and this variation depends on the transitions.

4 Theoretical analysis

4.1 Semi-classical impact models

In the framework of the Anderson-Tsao-Curnutte (ATC) theory the pressure-broadened line width (HWHM) of a single absorption line in cm^{-1}/atm is

$$\Delta\nu = \frac{Nv\sigma_r}{2\pi c} \tag{3}$$

where,

$N =$ number density of colliding molecules/atm,
$v =$ average relative velocity of the colliding molecules,
$\sigma_r =$ total collision cross-section and
$c =$ velocity of light.

The total collision cross-section σ_r for an absorbing molecule with initial state J_i and final state J_f is given as the sum of partial collision cross-sections σ_{J_2} weighted by population probabilities ρ_{J_2} of the states J_2 of the perturbing molecule,

$$\sigma_r = \sum_{J_2} \rho_{J_2}\sigma_{J_2}. \tag{4}$$

Here,

$$\rho_{J_2} = \frac{hcB_0}{kT}(2J_2+1)\,\exp\left[-\frac{hcB_0}{kT}J_2(J_2+1)\right] \tag{5}$$

and B_0 is the rotational constant of the perturber in the ground vibrational state. In our case the absorber and perturber molecules have no permanent dipole moments. So the interaction potential for the collision process arises mainly from quadrupolar (Φ_q) and dispersion (Φ_d) interactions defined by Buckingham [1] for interaction of two linear molecules in terms of the quadrupole moments q, polarizability α, anisotropy of polarizability $(\alpha_\parallel - \alpha_\perp)/\alpha$, first ionization potential U, the relative configuration of the molecules and the intermolecular separation. The contribution from the vibrational dephasing effect for isotropic part of the potentials has been neglected for weak interaction phenomena in the combination overtone band transition in our calculation. The partial cross-section σ_{J_2} may be obtained as

$$\sigma_{J_2} = \int_0^\infty 2\pi b\,\mathrm{d}b\; S(b). \tag{6}$$

The impact parameter b is defined as the distance of the closest approach of the colliding molecules. $S(b)$ defines the probability of the collision induced transition of the absorbing molecule for a certain b value. Considering the order of perturbation terms of the collisional Hamiltonian, the first order term $S_1(b)$ is imaginary and leads to line shift while the second order term $S_2(b)$ gives rise to line width.

In the Anderson cutoff procedure the probability function $S_2(b)$ has a maximum value of unity for all values

$$S_2(b) = A_q b^{-8}\left[\sum_{J_i' J_2'} Q_1(J_i J_i') Q_2(J_2 J_2') f_3(k) + \sum_{J_f' J_2'} Q_1(J_f J_f') Q_2(J_2 J_2') f_3(k) + B\sum_{J_2'} Q_2(J_2 J_2') f_3(k)\right]$$
$$+ A_{d1} b^{-10}\left[\sum_{J_i'} Q_1(J_i J_i') g_1(k) + \sum_{J_f'} Q_1(J_f J_f') g_1(k) + B\right]$$
$$+ A_{d2} b^{-10}\left[\sum_{J_i' J_2'} Q_1(J_i J_i') Q_2(J_2 J_2') g_2(k) + \sum_{J_f' J_2'} Q_1(J_f J_f') Q_2(J_2 J_2') g_2(k) + B\sum_{J_2'} Q_2(J_2 J_2') g_2(k)\right] \quad (8)$$

of b less than a certain value b_0. In this case σ_{J_2} can be written as

$$\sigma_{J_2} = \pi {b_0}^2 + \int_{b_0}^{\infty} 2\pi b \,\mathrm{d}b \; S_2(b). \quad (7)$$

The probability function $S_2(b)$ arising from quadrupolar and dispersion terms [23] is

see equation (8) above.

Here, J_i', J_f' and J_2' denote collision induced states.

$$A_\mathrm{q} = \frac{16}{25}\left(\frac{q_1 q_2}{\hbar v}\right)^2, \quad (9)$$

$$A_\mathrm{d1} = \frac{84\,\pi^4}{10240}\left[\frac{U_1 U_2}{U_1 + U_2}\frac{(\alpha_\parallel - \alpha_\perp)_1 \alpha_2}{hv}\right]^2, \quad (10)$$

$$A_{d2} = \frac{2236\,\pi^4}{1228800}\left[\frac{U_1 U_2}{U_1 + U_2}\frac{(\alpha_\parallel - \alpha_\perp)_1 (\alpha_\parallel - \alpha_\perp)_2}{hv}\right]^2. \quad (11)$$

All Q-terms involved in (8) are the transition probabilities for the transitions $\Delta J = 0, \pm 2$

$$Q(J, J+2) = \frac{3}{2}\frac{(J+1)(J+2)}{(2J+1)(2J+3)}, \quad (12)$$

$$Q(J, J) = \frac{J(J+1)}{(2J-1)(2J+3)}, \quad (13)$$

$$Q(J, J-2) = \frac{3}{2}\frac{J(J-1)}{(2J-1)(2J+1)}. \quad (14)$$

The term B in equation (8) is given by

$$B = (-1)^{J_\mathrm{i}+J_\mathrm{f}}\, 2\Big[(2J_\mathrm{i}+1)(2J_\mathrm{f}+1) Q_1(J_\mathrm{i}, J_\mathrm{i}) Q_1(J_\mathrm{f}, J_\mathrm{f})\Big]^{1/2} \times W(J_\mathrm{i} J_\mathrm{f} J_\mathrm{i} J_\mathrm{f}, 12) \quad (15)$$

and the Racah's coefficient is given by

$$W(J_\mathrm{i} J_\mathrm{f} J_\mathrm{i} J_\mathrm{f}, 12) = \frac{(-1)^{2J}\,[(2J+5)(J+2)J(2J-1)]^{1/2}}{(J+1)(2J+1)(2J+3)} \quad (16)$$

where, $J = J_\mathrm{i}$ for R-branch and $J = J_\mathrm{f}$ for P-branch. $f_3(k)$, $g_1(k)$ and $g_2(k)$ are the off-resonance functions [2,4], $f_3(k)$ has the values tabulated in reference [4]

$$g_1(k) = \frac{\mathrm{e}^{-2k}}{63}\left[2k^6 + 12k^5 + 39k^4 + 84k^3 + 126k^2 + 126k + 63\right] \quad (17)$$

$$g_2(k) = \frac{\mathrm{e}^{-2k}}{5031}\left[54k^8 + 216k^7 + 668k^6 + 1740k^5 + 3876k^4 + 7176k^3 + 10296k^2 + 10062k + 5031\right] \quad (18)$$

where

$$k = \frac{2\pi c}{v}\, b\, \Delta E. \quad (19)$$

ΔE is the off-resonance energy. The value of ΔE is calculated as the difference between the gain of the energy of the absorber molecule and the loss of energy of the perturber molecule in each collision process. The final state of the absorber molecule is the upper vibrational state while both states of the perturber molecule are the ground vibrational state. For a certain rovibrational transition, we can calculate ΔE for the states of the perturber molecule with $J_2 = 0$ and higher values. The value of ΔE depends upon the rotational constants B_0 and B_v for the absorber and B_0 for the perturber and on the rotational quantum numbers J_2, J_i and J_f.

We shall terminate our calculation of the ΔE values for different J_2 values upto $J_2^{\max}$ where $\sigma_{J_2^{\max}}$ attains a constant value. Thus $\sigma_{J_2^{\max}}$ is the lowest value of the collision cross-section. Hence

$$\sigma_r = \sum_{J_2=0}^{J_2^{\max}} \rho_{J_2}\sigma_{J_2} + \left(1 - \sum_{J_2=0}^{J_2^{\max}} \rho_{J_2}\right)\sigma_{J_2^{\max}}. \quad (20)$$

A computer program has been developed for calculation of b_0 and half width. In order to calculate b_0 by Anderson cutoff procedure we have to solve the equation $S_2(b_0) = 1$ where $S_2(b)$ is given by (8). After calculation of ΔE we calculate the value of k with a trial value of b. With values of $f_3(k)$ from reference [4] and $g_1(k)$ and $g_2(k)$ from (17, 18) we evaluate $S_2(b)$ and minimize $[S_2(b) - 1]$

by changing b. The corresponding b is taken as b_0. These values of b_0 are used in the calculations of σ_{J_2} from (7–19). If b_0 is less than the kinetic collision diameter r_0, its value is replaced by r_0. The integrals of $f_3(k)$ lead to the function $F_3(k)$ tabulated in reference [4] and k_0 corresponds to b_0 (Eq. (19)); the integrals of $g(k)$ are calculated numerically as suggested in the reference [4].

The difficulty for cutoff of the $S_2(b)$ curve at $b = b_0$ has been bypassed in the Murphy-Boggs (MB) [24] model which calculates the collision probability $\Gamma_{J_1J_2}$ associated with the transition $J_1 \longrightarrow J_2$ and the line width can be expressed in terms of $\exp(-\Gamma_{J_1J_2})$. $\Gamma_{J_1J_2}$ contains the interruption function $S_2(b)$. In the MB model also $S_2(b)$ is unity for low values of b since the two molecules cannot approach closer than the sum of the radii of the molecules at the moment of collision. However, this model allows a smooth variation of $S_2(b)$ in going from higher to lower b values and avoids forced joining of the two curves. Result of this procedure is that the calculation allows somewhat lower values of b_0 than the Anderson procedure. Hence the calculated values of line widths would be lower than those obtained with the ATC model, even when the same interactions are considered in the two cases. Further, the MB model does not include all of the non-resonant terms in the interaction matrix as in case of ATC model.

Another semi-classical molecular line broadening theory [25] developed by Robert and Bonamy is useful to include the effect of short range repulsive intermolecular potential in absence of higher order multipole moments of colliding molecules for diatom-atom, atom-atom collisions and so on. This model also permits smooth variation of collision probability function but the relative dependence of multipolar interactions on the impact parameter as well as line width cannot be estimated precisely. So in presence of quadrupole moments of acetylene and its collision partners we prefer ATC model to include the orientation effect of colliding molecules in the impact parameter and to obtain the quantum number dependence with sufficient accuracy [26]. Apart from these factors both the methods are based upon impact theory. The results obtained so far with both the theories do not conclusively show the superiority of one model over the other.

4.2 Self-broadening calculations

A detailed calculation of half width in the ATC model is carried out with the parameters given in Table 2. It should be mentioned that the exact spectroscopic source values of quadrupole moment and anisotropy in polarizability of the active molecule are quite unknown in our case. The value of the quadrupole moment of acetylene is obtained from microwave line broadening perturbed by ammonia [27]. In an earlier calculation a higher value of $4.0d$ Å was obtained by adjusting the value of the observed half width in the IR region [33]. We have used both the values for comparison with experimental data on self-, N_2- and O_2-broadened line width. The information on polarizability and other parameters are available from the literature (Tab. 2). For the kinetic collision diameter it may be noted that the linear dimension d_0 of acetylene is 4.22 Å. Hence in the case of self-collision when the two molecules collide along the length of the molecules the value of r_0 may be taken as 4.22 Å. However, in the case of collision in the perpendicular or T-configuration the length may be taken approximately as $(4.22 + 1.0)/2 = 2.61$ Å. Since all collision configurations are possible in the gas phase we assume an average kinetic collision diameter of 3.42 Å. Since the interaction potential is weak the b_0 value obtained is usually smaller than $4.0d$ Å, hence if r_0 is assumed as 4.22 Å, most of the collision processes will use this value of r_0 in place of b_0. This would lead to gross overestimation of line width even when $q = 3.0d$ Å.

Table 2. Molecular parameters used in the calculations.

Parameters	C_2H_2	N_2	O_2
q (d Å)	3.00 [a]	1.52 [b]	0.39 [b]
$\alpha_\parallel \times 10^{25}$ (e.s.u.) [c]	51.2	23.8	23.5
$\alpha_\perp \times 10^{25}$ (e.s.u.) [c]	24.3	14.5	12.1
$\alpha \times 10^{25}$ (e.s.u.) [c]	33.3	17.6	16.0
$U \times 10^{11}$ (erg) [d]	1.1400	1.5576	1.2063
B_0 (cm^{-1})	1.17692 [e]	1.98962 [f]	1.43765 [g]
B_v (cm^{-1})	1.15096 [h]	—	—
d_0 (Å) [c]	4.221	3.698	3.580

[a] Ref. [27], [b] Ref. [28], [c] Ref. [29], [d] Ref. [30], [e] Ref. [9], [f] Ref. [31], [g] Ref. [32], [h] Ref. [12].

As mentioned earlier we have retained all the non-resonant interactions upto a certain value of J_2. For higher J_2 the values of b_0 become very small. For each value of J_2 we solve $S_2(b_0) = 1$ to obtain b_0 as described earlier. For $q_1 = 3.0d$ Å the value of b_0 varies between a maximum value of 3.95 to a minimum value of 3.42 Å. If only quadrupolar interactions are taken into account they are further smaller because of smaller interactions. For $q_1 = 4.0d$ Å most of the b_0 values are higher than 4.22 Å. The solutions of the equation $S_2(b_0) = 1$ are to be continued upto those non-resonant cases where b_0 attains the value r_0. However, the calculation of σ_{J_2} is to be continued with $b_0 = r_0$ till $J_2^{\max}$ where σ_{J_2} attains a constant value and does not decrease further.

In order to find the relative effect of the two potential terms on the line width we have to calculate the relative magnitude of the two interaction terms in $S_2(b)$. The contributions of the dispersion terms in $S_2(b_0)$ for different J_2 values are shown in Figure 5. It is evident from the figure that for the self-collision problem the dispersion term can have a contribution of approximately 60% in the nearly resonant cases with $J_2 = 11$ for the P13 transition. For higher J_2 it drops rapidly, so the quadrupolar contribution increases since their sum is unity and hence it has larger effect on the line width. For higher values of quadrupole moment the quadrupolar part has a larger role for all J_2 values. In such cases b_0 is usually higher than r_0 so that we have a strong interaction case. For lower q-values the dispersion terms are more important. In the ATC model if only quadrupolar interactions are considered we get

Table 3. Self and nitrogen-broadening coefficients Γ/P ($cm^{-1}atm^{-1}$) in the ($\nu_1 + 3\nu_3$)band of C_2H_2 for different values of quadrupole moment (q) in d Å.

Transition	self			nitrogen		
	Obs.[a]	Cal.		Obs.[a]	Cal.	
		$q_1 = 3.0$	$q_1 = 4.0$		$q_1 = 3.0$	$q_1 = 4.0$
P7	0.0996(14)	0.0773	0.0942	0.0803(4)	0.0530	0.0567
P8	0.0822(6)	0.0790	0.0960	0.0604(5)	0.0543	0.0581
P13	0.0874(2)	0.0837	0.1012	0.0736(5)	0.0597	0.0638
P15	0.0612(4)	0.0835	0.1011	0.0532(5)	0.0609	0.0651
R9	0.1138(5)	0.0825	0.0996	0.0910(4)	0.0576	0.0615
R11	0.0901(6)	0.0841	0.1015	0.0874(2)	0.0594	0.0634

[a]Ref. [5]

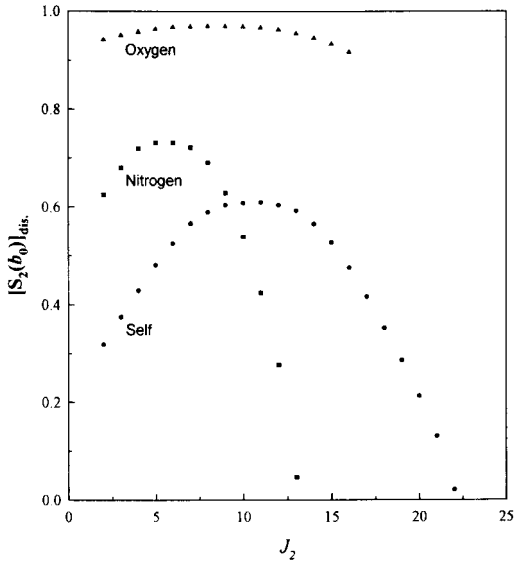

Fig. 5. Dependence of the $[S_2(b_0)]_{\text{dis.}}$ on the quantum number J_2 in the ($\nu_1 + 3\nu_3$) band P13 transition of C_2H_2 for the self, nitrogen and oxygen broadening cases.

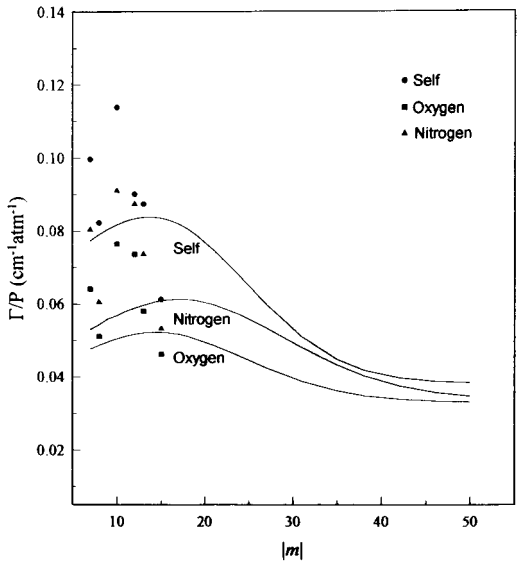

Fig. 6. Plot of Γ/P calculated from the ATC model against $|m|$ for different perturbers. The observed values are also shown with different symbols.

somewhat lower values of b_0, but the calculated line width is close to that obtained by considering both the interactions since the effects on the line width of these two interactions considered separately are not simply additive. Hence the relative magnitudes cannot be calculated by considering the two interactions separately [4].

The calculated values of collisional broadening coefficient Γ/P (Tab. 3) show that the agreement with the observed values is better for the value of $q_1 = 3.0d$ Å; the values are somewhat larger for $q_1 = 4.0d$ Å. For the $q_1 = 3.0d$ Å case the calculated values exhibit very little dependence on J_i in the range of measurement. The small dependence on J_i values arises from the fact that b_0 varies slowly with J_2. It is verified that the calculated half width is almost unchanged if an average value of b_0 is used. In this case the first part of $S_2(b)$ in (7) is independent of J_2; so the total collision cross-section σ_r (Eq. (4)) arising from this part is $\pi {b_0}^2$ because $\sum_{J_2} \rho_{J_2} = 1$. It is found that for an average value of $b_0 = 3.69$ Å the calculated half width from the first term in (7) is nearly equal to 0.0606 cm^{-1} and is independent of the transition. Hence the J_i dependence which arises only from the second integral term of (7) is small. Previous calculations of line width by the ATC model also show small variations with J_i values of the absorber [33,34]. The curve in Figure 6, for the calculated line broadening parameter Γ/P for different $|m|$ values (where $m = -J_i$ for P-branch and $m = J_i + 1$ for R-branch) shows variation of Γ/P over a long range of J_i values. Here it is noticeable that the Γ/P value for lower J_i's show a small increase and then it goes on decreasing for very high J_i [34]. In such cases the second term of (7) has an important role. It may be further noted that the contributions of the non-resonant terms with J_2 greater than $J_2^{\max}$ are small. This value of $J_2^{\max}$ varies with the transitions. For P7 transition $J_2^{\max} = 44$ while for higher J_i values it becomes larger. It is found that by retaining terms upto $J_2^{\max}$ we can include upto 99% of the occupied

energy levels in the summation over J_2. The rest of the energy levels have a constant contribution of only 1%.

4.3 Nitrogen and oxygen-broadening

Similar calculations have been carried for broadening caused by collisions with N_2 and O_2 which have much smaller quadrupole moments (Tab. 2). This leads to smaller Γ/P values (Tabs. 1 and 3) in agreement with experimental results. In these cases the molecular diameters are also smaller (Tab. 2) than the self-broadened case. As in the self-broadened case average kinetic collision diameters for C_2H_2–N_2 and C_2H_2–O_2 are taken to be 3.17 and 3.11 Å respectively. The calculated values of b_0 are also smaller. It is found (Fig. 5) that the dispersion term will have almost 73% contribution in the nearly resonant case with $J_2 = 6$ for the P13 transition for the N_2-broadening case and will have almost 97% contribution in the nearly resonant case with $J_2 = 8$ for the same transition for the O_2-broadening case. Because of very small value of quadrupolar moment of O_2, the dispersion term plays a dominant role in the calculation of b_0 and shows very small change with J_2. The shift in the value of J_2 for the nearly resonant cases is consistent with the variation of mass of the perturber molecules. It is verified that the contributions to the half width σ_r from the πb_0^2 term for average values of $b_0 = 3.335$ and 3.200 Å are 0.0486 and 0.0434 cm^{-1} for the N_2 and O_2 collisions respectively. It is also found that the value of σ_{J_2} attains a constant small value at much lower values of $J_2^{\max} = 29$ and 36 for N_2- and O_2-broadening cases respectively. This is due to variation of rotational constants causing a difference to the rate of off-resonance interaction occurring for different perturber molecules. As in the self-broadening case the variation of the calculated half width with changes of J_i values in the range 9 to 15 is small and is in conformity with experiment. But it is found that the calculated half width is much smaller for high J_i values. Similar result was also found earlier by Bouanich *et al.* [33].

4.4 Air-broadening

We have calculated the air-broadened half width (Tab. 1) for the same transitions from the expression

$$\Gamma_{\text{air}} = p_{N_2}\Gamma_{N_2} + p_{O_2}\Gamma_{O_2}. \quad (21)$$

These results are compared with the values observed by direct measurement with air as a perturber. These values are also close to those computed from separate observed results for N_2 and O_2 perturbations (Tab. 1). Agreement of the calculated and observed values is similar to the earlier cases.

5 Conclusions

In this work we have reported NIR diode laser spectroscopic measurement of O_2 and air-broadening of the rotational components of the acetylene ($\nu_1 + 3\nu_3$) band transitions. Measurements for the same transitions for self- and N_2-broadening cases were reported earlier [5]. The pressure broadening coefficients and line strength parameters are obtained by simulation and fitting with the Voigt profiles. Both Γ/P and S values are affected by the perturbers. The measured values of S in presence of air for P13 and P15 transitions differ from the values measured in presence of oxygen. For air broadening measurements the air from the laboratory atmosphere is directly introduced in the sample cell. Any impurity which may have absorptions at wavelengths close to some of the acetylene transitions may affect the values of S and Γ/P for the air broadening case. However, the large deviation of S values for the different perturbers cannot be fully explained at this stage. The change of Γ/P with perturber has been theoretically calculated. We have attempted theoretical calculations of half width for all the cases with the impact approximation method of Anderson. In the ATC model calculation of half width the value of b_0 has a deterministic part. The determination of b_0 depends on the potential function used in the calculation. By allowing lower b_0 values arising from the effect of orientation of the perturber relative to the absorber in the ATC calculation our calculated half widths are smaller and are closer to the observed values. It is pointed out that in case of collisions of two linear molecules the distance of closest approach of the two molecules is not the same for every collision and should depend on the collision configuration. One can thus consider an average distance of closest approach which in our self-broadened case is much lower than 4.22 Å. Thus in spite of sharp joining of the two curves in the ATC procedure we allow larger contributions of the integral in (7) and larger J_i dependence. It may be mentioned that the calculated half width has little dependence on the smoothness of joining the two curves, but it depends strongly on how much we allow the two molecules to come closer to each other. It may be mentioned here that a recent study of interaction of fast molecular ions He^+ with N_2 molecule [35] shows strong orientation effect of molecular alignment on multiple ionization of the molecule. This effect arising from the anisotropy of electron density distribution is analogous to our case of collision of two linear molecules.

In our calculation we have restricted to quadrupolar and dispersion interactions only and all higher order multipolar interactions are neglected. Although these interactions are small, they could add to the calculated values. This justifies that our calculated values are lower than the observed values. The half widths have lower values for high J_i. For low J_i values where measurements are carried out the calculated values are close to the observed ones. But the J_i-dependence is not reproduced. This may arise from the weakness of the impact approximation. Moreover, the energy levels for these higher vibrational states may also be considerably perturbed as the level density of the absorber molecule is too high in these regions. We have shown the relative contributions of the quadrupolar and dispersion terms on the collision perturbations by explicit calculations in all cases. It is found that for these weak

interaction cases dispersion terms have a large contribution to the line width. Most of the previous calculations with the ATC model were performed for strong interaction cases where one of the molecules has a dipole moment [31,32].

We have verified by explicit calculation that b_0 varies slowly with J_2 except for very high J_2 when population probability becomes smaller. It is also found that the line width calculated with an average b_0 is almost the same as that calculated with variable b_0 values. The results of Tables 1 and 3 show that in most cases the entire calculation in the ATC framework culminates in the determination of b_0 and the integral over b for $b \geq b_0$ has small contribution to the line width. Thus the calculated width has very small dependence on the transitions for low J values.

D.B. and B.R. thank the University Grants Commission, New Delhi for Research Fellowships. Financial assistance from the Department of Science and Technology (SP/S2/L–05/96) is gratefully acknowledged.

References

1. A.D. Buckingham, Adv. Chem. Phys. **12**, 107 (1967).
2. D. Robert, M. Giraud, L. Galatry, J. Chem. Phys. **51**, 2192 (1969).
3. P.W. Anderson, Phys. Rev. **76**, 647 (1949).
4. C.J. Tsao, B. Curnutte, J. Quant. Spectrosc. Radiat. Transfer **2**, 41 (1962).
5. D. Biswas, B. Ray, S. Dutta, P.N. Ghosh, Appl. Phys. B **68**, 1125 (1999).
6. P. Varanasi, L.P. Giver, F.P.J. Valero, J. Quant. Spectrosc. Radiat. Transfer **30**, 497 (1983).
7. P. Varanasi, L.P. Giver, F.P.J. Valero, J. Quant. Spectrosc. Radiat. Transfer **30**, 505 (1983).
8. P. Varanasi, J. Quant. Spectrosc. Radiat. Transfer **47**, 263 (1992).
9. G. Herzberg, *Infrared and Raman Spectra of Polyatomic Molecules*, 1st edn. (van Nostrand, New York, 1945).
10. R.R. Hall, Ph.D. thesis, Rice University, Houston, TX, 1984.
11. B.C. Smith, J.S. Winn, J. Chem. Phys. **94**, 4120 (1991).
12. X. Zhan, L. Halonen, J. Mol. Spectrosc. **160**, 464 (1993).
13. F.S. Pavone, F. Marin, M. Inguscio, K. Ernst, G. Di Lonardo, Appl. Opt. **32**, 259 (1993).
14. A. Lucchesini, M. De Rosa, D. Pelliccia, A. Ciucci, C. Gabbanini, S. Gozzini, Appl. Phys. B **63**, 277 (1996).
15. R.H. Dicke, Phys. Rev. **89**, 472 (1953).
16. B. Ray, P.N. Ghosh, Spectrochim. Acta A **53**, 537 (1997).
17. J. Reid, J. Shewchun, B.K. Garside, E.A. Ballik, Appl. Opt. **17**, 300 (1978).
18. K. Hedfeld, P. Lueg, Z. Phys. **77**, 446 (1932).
19. A.K. Hui, B.H. Armstrong, A.A. Wray, J. Quant. Spectrosc. Radiat. Transfer **19**, 509 (1977).
20. P.R. Bevington, *Data Reduction and Error Analysis for the Physical Sciences* (McGraw Hill, New York, 1969), p. 235.
21. D. Biswas, B. Ray, P.N. Ghosh, Chem. Phys. Lett. **275**, 314 (1997).
22. B. Ray, D. Biswas, P.N. Ghosh, J. Mol. Struct. **407**, 39 (1997).
23. Krishnaji, V. Prakash, Rev. Mod. Phys. **38**, 690 (1966).
24. J.S. Murphy, J.E. Boggs, J. Chem. Phys. **47**, 691 (1967).
25. D. Robert, J. Bonamy, J. Phys. **40**, 923 (1979).
26. J. Waschall, Y. Heiner, B. Supmf, H.-D. Kronfeldt, J. Mol. Spectrosc. **190**, 140 (1998).
27. R.M. Hill, W.V. Smith, Phys. Rev. **82**, 451 (1951).
28. D.E. Stogryn, A.P. Stogryn, Mol. Phys. **11**, 371 (1966).
29. J.O. Hirschfelder, C.I. Curtiss, R.B. Bird, *Molecular Theory of Gases and Liquids*, 1st edn. (Wiley, New York, 1954).
30. *CRC Handbook of Chemistry and Physics*, edited by R.C. Weast, 58th edn. (CRC Press, Florida, 1977–78).
31. D. Reuter, D.E. Jennings, J.N. Brault, J. Mol. Spectrosc. **115**, 294 (1986).
32. T. Amano, E. Hirota, J. Mol. Spectrosc. **53**, 346 (1974).
33. J.P. Bouanich, D. Lambot, G. Blanquet, J. Walrand, J. Mol. Spectrosc. **140**, 195 (1990).
34. G.D.T. Tejwani, J. Chem. Phys. **57**, 4676 (1972).
35. U. Werner, N.M. Kabachnik, V.N. Kondratyev, H.O. Lutz, Phys. Rev. Lett. **79**, 1662 (1997).